Finite Element Computation of Field, Forces and Inductances in Underground SF_6 Insulated Cables Using a Coupled Magneto-Thermal Formulation

D. Labridis and V. Hatziathanassiou

Abstract—**A finite element (FE) iterative formulation has been used for the computation of the coupled magneto-thermal field in underground SF_6 insulated high voltage cables. The formulation takes into account the real geometrical and physical properties of the involved materials. Using the field distributions, the cable ampacity and losses, the forces and the inductances have been calculated for both isolated phase and three-conductor arrangements. The influence of the operating parameters on these quantities is examined.**

I. Introduction

THE concentration of load in large industrial and urban areas and the installation of large power plants close to this load leads to the transmission of higher electrical power. Coupled with the expected increase of the load and generation density is an increase of the continuous current of the system. Values of 6300–8000 A for bus bars in the voltage range up to 525 kV may be regarded as typical [1], and the components of the transmission system (bus bars, cables, circuit breakers) have to support and control the normal and short circuit currents. SF_6 insulated underground power cables may be used for the transmission of this high electrical power for short station getaways and underpasses, because they have advantages compared with traditional oil-impregnated or oil-filled pipe type cables [2], [3]. Therefore, the calculation of the operating parameters of gas insulated cables (including electromagnetic and thermal fields, losses, forces and inductances) is of importance for the design and reasonable operation of the transmission system.

The finite element method (FEM) has been used extensively in the solution of thermal problems [21]–[22] in underground cables as well as of eddy-current multiconductor problems [4], [6], [11], [23]. The first attempts to couple the two problems were made by approximating the cable geometry and neglecting the skin and proximity effects in [24] or by assuming the electric conductivity independent of temperature in [7].

In [3] a FE iterative formulation has been presented for the computation of the coupled magneto-thermal field in underground SF_6 insulated cables. In this paper, the formulation of [3] has been extended to model the electromagnetic and thermal steady-state diffusion problems in both isolated phase and three-conductor gas insulated cables. As a result, the field distributions of the magnetic vector potential (MVP) and of the temperature can be calculated. The ac losses, the forces acting on the conductors as well as their inductances are formulated, using the MVP distribution. The cable ampacity is also estimated from the temperature distribution, using a given maximum sheath temperature as a limitation. The assumptions that were used in the calculation are the following.

- The cable is of infinite length, so that the coupled diffusion problem becomes a two-dimensional one;
- Charges and displacement currents are neglected;
- The conductors and the sheaths have constant relative magnetic permeabilities μ_{rc} and μ_{rs} respectively;
- The electrical conductivities, σ_c and σ_s of the conductor and sheath are functions of temperature;
- The thermal conductivities of the conductors, sheaths, soil and backfill (k_c, k_s, k_e and k_b, respectively) are independent of temperature;
- The air inside the tubular conductors is stationary, therefore the thermal conductivity of air k_a is used in this region;
- An effective thermal conductivity k_{eff} of SF_6, including the effects of free convection and radiation between conductor and sheath, is calculated. Conduction becomes the dominant mode of heat transfer in the whole domain. This effective thermal conductivity k_{eff} is a function of the mean temperatures of the sheath and conductor. The phase currents are sinusoidal and balanced, therefore complex functions for the time variation of the three conductor currents may be used.

II. The Electromagnetic Field Problem

A. Electromagnetic Diffusion and Boundary Conditions

The assumptions made lead to a piecewise linear, steady-state, time harmonic electromagnetic field in a two-dimensional region S bounded by the curve C. Supposing that the region S lies on the x-y plane and following the analysis presented in [3], the two-dimensional electro-

Manuscript received July 9, 1993; revised February 7, 1994.

The authors are with the Department of Electrical Engineering, Aristotelian University, Thessaloniki, P.O. Box 486, GR-54006 Thessolonica, Greece.

IEEE Log Number 9401377.

magnetic diffusion problem for the z-direction components of the MVP, A_z, and of the total current density vector, J_z, is described by the system of equations

$$\frac{1}{\mu_0\mu_r}\left[\frac{\partial^2 A_z}{\partial x^2}+\frac{\partial^2 A_z}{\partial y^2}\right]-j\omega\sigma A_z+J_{sz}=0$$

$$-j\omega\sigma A_z+J_{sz}=J_z \qquad \text{(1a)}$$

the boundary conditions

$$A_z|_C = A_0(x, y) \qquad \text{(1b)}$$

and the integral form

$$\int\int_S J_z\, ds = I_{rms}, \qquad \text{(1c)}$$

where μ_0 is the magnetic permeability of vacuum, μ_r is the relative magnetic permeability, J_{sz} is the z component of the uniformly distributed source current density and I_{rms} is the rms of the current flowing through each conductor. The unknowns in the system of (1a) are A_z and J_{sz}, while the values of A_z at the limit C of region S are specified by the Dirichlet condition (1b) and the total current density J_z is specified in the integral form (1c).

B. Finite Element Formulation

The conductivity $\sigma(T)$ of a material at T°C, according to the assumptions, is approximated by

$$\sigma(T)=\frac{\sigma_0}{1+\alpha T} \qquad (2)$$

where σ_0 is the conductivity at 0°C and α is the temperature coefficient of this material.

Applying the Galerkin method to the system of equations (1), assembling the element contributions in the usual way [4] and taking into account the temperature dependence of the conductivity, the following matrix equation is obtained

$$\begin{bmatrix} \frac{1}{\mu_0\mu_r}\mathbf{S}_F - j\omega\sigma(T)\mathbf{T}_F & -j\omega\sigma(T)\mathbf{Q} \\ -j\omega\sigma(T)\mathbf{Q}^t & j\omega\sigma(T)\mathbf{W} \end{bmatrix}\begin{bmatrix}\mathbf{A}\\ \mathbf{G}\end{bmatrix}=\begin{bmatrix}\mathbf{0}\\ \mathbf{I}\end{bmatrix} \qquad (3)$$

where S_F and T_F are the usual *FE* matrices encountered in the solution of eddy current problems [5], while the vectors Q, I, and G and the diagonal matrix W are defined in [6] for the multiconductor FE formulation.

III. The Temperature Field Problem

A. Gas Insulated Cables—Effective Thermal Conductivity of the Insulation Gas

1) Isolated Phase Gas Insulated Cables: Explicit ampacity equations may only be derived when the radial temperature drops are proportional to heat flux, as in thermal conduction. In gas insulated cables the heat must be transferred across two surfaces in series, i.e., the outside of the conductor's and the inside of the sheath's surface. So both free convection and radiation are important and the ampacity must be determined by successive approximations. Conduction is the dominant mode of heat transfer from the sheath outward. In order to define an effective thermal conductivity that takes into account both free convection and radiation from the conductor's to the sheath's surface, the following formulae were used

If T_c and T_s are the mean temperatures of the conductor and sheath, respectively, then the temperature drop across a concentric fluid gap may be expressed as

$$T_c - T_s = \frac{Q \ln (R_i/r_o)}{2\pi k_{\text{eff}}} \qquad (4)$$

where Q is the heat flow per unit length (W/m), k_{eff} is the effective thermal conductivity (W/m°C), R_i is the inner sheath radius (m) and r_o is the outer conductor radius (m). In order to calculate k_{eff} from (4), the total heat flow per unit length Q must be known. This total heat is the sum

$$Q = Q_r + Q_c \qquad (5)$$

of the radiation and convection heat flows, Q_r and Q_c, respectively.

The Stephan–Boltzman law for a coaxial line gives the radiation heat flow Q_r per unit length as

$$Q_r = 5.67\times 10^{-12}\times 2\pi r_o \xi'[(273+T_c)^4-(273+T_s)^4] \qquad (6a)$$

where [8]

$$\xi' = \frac{\xi_c\xi_s}{\xi_s+(R_i/r_o)(1-\xi_s)\xi_c}. \qquad (6b)$$

The emissivities ξ_c and ξ_s of conductor and sheath that appear in (6b) depend on their electrical conductivity. Assuming that the conductors are made of EC grade aluminum and the enclosure pipes of some high-strength aluminum alloy, it is recommended to use the values $\xi_c = 0.3$ and $\xi_s = 0.8$ [2].

Considering now the convective heat flow Q_c per unit length, we must take into account its dependence on the gas density and therefore on the gas pressure and temperature. For an SF_6 insulated cable that has been filled to 345 kPa (50 psi) at 20°C, which is typical for isolated phase systems, Doepken [9] recommends the following formula for convection

$$Q_c = \frac{3.75\times 10^{-3}(T_c-T_s)^{1.2}(R_i-r_o)^{0.6}}{\ln (R_i/r_o)} \qquad (7)$$

2) Three-Conductor Gas Insulated Cables: When the three conductors are inside the same gas-filled enclosure, a further simplifying assumption has to be made about the heat transfer through the gas insulation. For this reason we may consider an imaginary cylindrical heat dissipation surface of radius R_e, as shown in Fig. 2(a). This is an envelope of the three conductors and should be considered

to consist of the same material as the conductors. Around this envelope's periphery the three conductors' Joule losses emanate uniformly. Using this assumption we deal again with the heat transfer problem across a concentric fluid gap, so the effective thermal conductivity k_{eff} of this gap may be calculated from the relations (4) to (6) if we use the envelope's radius R_e instead of r_o.

B. Thermal Diffusion and Boundary Conditions

Under steady-state conditions, the differential equation governing the heat conduction is

$$-k\left[\frac{\partial^2 T}{\partial x^2}+\frac{\partial^2 T}{\partial y^2}\right]=\dot{q} \tag{8a}$$

where $\dot{q}$ is the rate of heat generated per unit volume per unit time and k is the thermal conductivity. The corresponding boundary conditions are

$$T|_{C_1}=T_0(x, y) \tag{8b}$$

and

$$k\left[\frac{\partial T}{\partial x}l_x+\frac{\sigma T}{\partial y}l_y\right]+q_s+h(T-T_\infty)=0 \quad \text{on } C_2 \tag{8c}$$

where C_1 is the boundary on which a prescribed temperature $T_0(x, y)$ is specified, l_x and l_y are the direction cosines of the outward normal to the surface and C_2 is the boundary on which both the heat flux q_s due to conduction and the convective heat loss $h(T-T_\infty)$ are specified, where h is the convection heat coefficient and T_∞ is the ambient temperature.

C. Coupled Finite Element Formulation

According to the assumptions, the effective thermal conductivity k_{eff} of SF_6 is a function of the mean conductor and sheath temperatures, T_c and T_s, respectively. The internal heat generation $\dot{q}$ is also a function of temperature. In order to calculate $\dot{q}$ for the typical finite element e we may use the relation [6]

$$\dot{q}^e=\frac{J^e J^{e*}}{\sigma^e} \tag{9}$$

where J^e and σ^e are the total current density and the electric conductivity of element e, respectively. The following remarks are made:

1) σ^e is explicitly dependent on temperature due to (2).
2) The MVP approximation of this element, $A^e(x, y)$, and the corresponding source current density, J_s^e, as they will be derived from the solution of (3), are implicitly dependent on temperature. If we assume a first-order triangular element e with local MVP nodal values A_1^e, A_2^e and A_3^e, then the total current density J^e may be calculated from [3]

$$J^e=-\frac{j\omega\sigma^e}{3}(A_1^e+A_2^e+A_3^e)+J_{si}. \tag{10}$$

Therefore J^e is also temperature dependent.

The above analysis, using the FEM formulation of the two-dimensional heat conduction problem, leads to the matrix equation

$$\sum_e [\mathbf{K}_1^e(T)+\mathbf{K}_2^e]\mathbf{T}=\sum_\epsilon [\mathbf{P}_1^e+\mathbf{P}_3^e] \tag{11}$$

where the matrices **K, P** and **T** are given in [3].

IV. Incorporation of the Boundary Conditions

The electromagnetic and thermal fields of both isolated phase and three-phase gas insulated cables may be considered unbounded. The FEM has been used to solve unbounded field problems using several different approaches, such as the extension of the discretization area (direct solution), the use of integral equations (Green's function) [16], the "window frame technique" [17], the boundary element method [18], the "infinitesimal scaling" [19] as well as the newer "hybrid harmonic/finite element method" [20].

For the reasons explained in [10], the first method was adopted here. Because the boundary conditions of the two diffusion problems have to be imposed on the same curve C, it is possible to use the same finite element mesh for both by simply defining the appropriate boundary conditions for the problem that is currently solved.

As shown in Fig. 1(b) and Fig. 2(b), the cables are buried in depth D from ground surface. The solution region S is bounded by the curve C, where $C = AB \cup B\Gamma \cup \Gamma\Delta \cup \Delta A$. The boundary conditions (8b) and (8c) of the thermal diffusion problem will be examined first. Boundary lines $B\Gamma$, $\Gamma\Delta$ and ΔA are of type C_1, while boundary line AB is of type C_2. The method of repeated solution of [10] leads to the conclusion that a mesh of 24 m width and 12 + D m depth (for both isolated phase and three-conductor gas cables) leads to zero heat flux in every point belonging to $C_{B\Gamma\Delta A}$. This mesh is practically unaffected by the heat sources of the problem and consequently satisfies both (8b) and (8c), corresponding to the imposed conditions

$$T|_{C_{B\Gamma\Delta A}}=T_{sp} \tag{12a}$$

$$k\left[\frac{\vartheta T}{\partial x}l_x+\frac{\vartheta T}{\partial y}l_y\right]+h(T-T_\infty)=0 \quad \text{on } C_{AB} \tag{12b}$$

where T_{sp} is the specified soil temperature.

The boundary conditions of the electromagnetic diffusion problem are the subject of the next question concerning the finite element mesh. A homogeneous Dirichlet condition obtained from (1b) has to be imposed on C. The distance of curve C from the cables has been estimated [6] as 5 to 6 times a typical dimension of the cable arrangement. This typical dimension is the sheath radius R_i in the case of a three phase gas cable and the distance $2S$ of the outer cables in the case of an isolated phase cable. Typical values for R_i are from 0.3 to 0.6 m and for S from 0.5 to 1.6 m, so the finite element mesh that has been already assumed for the satisfaction of the boundary conditions of the thermal problem automatically satisfies the electromagnetic boundary conditions. So along the

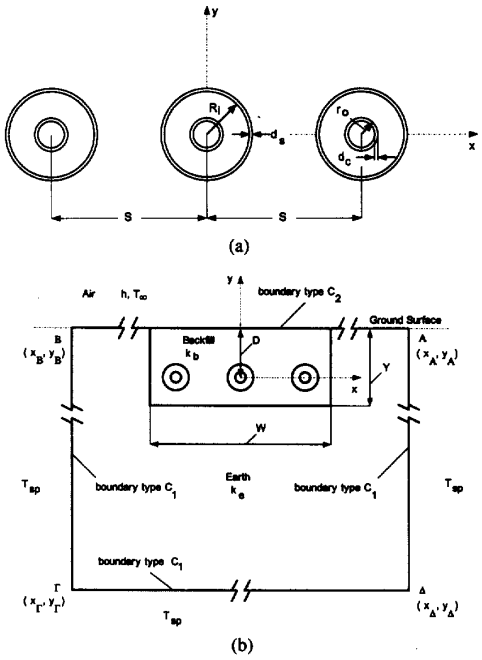

Fig. 1. Isolated-phase gas insulated cable: (a) Cross section of the three conductors, (b) Cable in trench and discretization area of the problem.

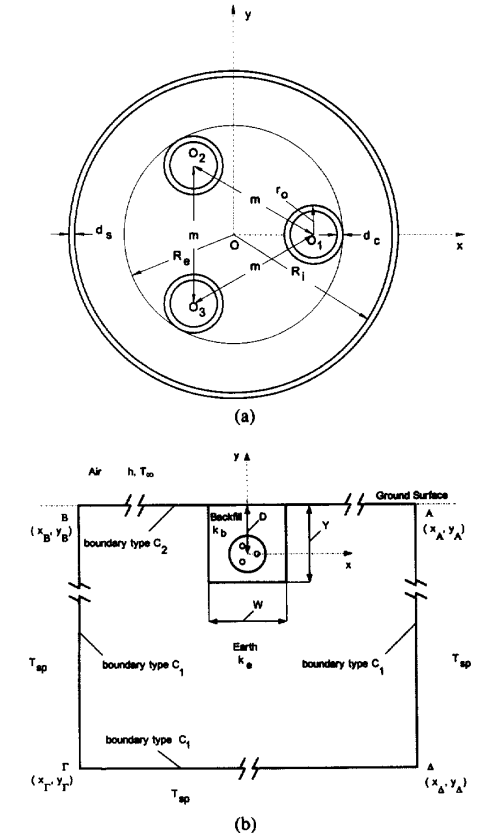

Fig. 2. Three conductor-one sheath gas isolated cable: (a) Cross section of the cable, (b) Cable in trench and discretization area of the problem.

boundary C of Fig. 1(b) and Fig. 2(b) the condition imposed is

$$A_z|_c = 0 \tag{13}$$

V. The Iterative Procedure

The computation of the MVP A and of the source current density J_s from (3) requires the determination of the rms current I_{rms}, in order to define the vector **I**. For the calculation of the electrical conductivity σ, the temperature distribution on the conductors and sheaths is also necessary. On the other hand, the computation of T from (11) requires the determination of the average loss density $\dot{q}$, to define the vector P_1. The effective thermal conductivity k_{eff} is also calculated using the mean temperatures of the conductors and of the sheaths, T_c and T_s, respectively. This problem is solved by an iterative procedure, consisting of the following 4 steps:

Step 1: The solution of (3) leads to the unknown values of MVP A at every node and of the source current density J_s at every conductor.

In the first iteration, the temperatures of the conductors and of the sheaths are set equal to arbitrary and constant values. For all the next iterations, the temperature values at every point will be obtained from step #4 and they will be different from point to point.

Then the electrical conductivities σ^e at every element e that lies on the cross-section of the conductors and of the sheaths are computed according to (2).

Step 2: Using the values of A and J_s from the solution at step #1, the total element current density J^e is computed from (10), if element e lies on the cross-section of conductor i having source current density J_{si}, or from

$$J^e = -\frac{j\omega\sigma^e}{3}(A_1^e + A_2^e + A_3^e) \tag{14}$$

if element e lies on the cross-section of the sheath. Using (10) or (14) and (9), the average loss density $\dot{q}^e$ of element e is calculated.

Step 3: Using the values of T from the solution in step #4, the mean conductor (T_c) and sheath (T_s) temperatures are calculated. Then, the effective thermal conductivity k_{eff} of SF_6 is computed from (4).

Step 4: The solution of (11) leads to the unknown values of T at every node. The values of i iteration $T_{(i)}$ are compared with the values $T_{(i-1)}$ of the previous iteration. If $|T_{(i)} - T_{(i-1)}| \leq T_{err}$ at every node, where T_{err} is a small temperature, the iterative procedure is terminated. The value of T_{err} used in the calculations of this paper was 1°C and the iterations needed in all cases were three or less.

VI. Calculation of Cable Operating Parameters

A. Losses and Inductances

The total ac losses per unit length of an isolated phase cable are equal to

$$P_t = \sum_{i=1}^{3}(P_{ci} + P_{si}) \tag{15}$$

where P_{ci} and P_{si} are the phase i ($i = 1, 3$) conductor and sheath losses per unit length respectively, while the total ac losses of a three-conductors one-sheath cable will be

$$P_t = \sum_{i=1}^{3} P_{ci} + P_s \tag{16}$$

where P_s are now the ac losses per unit length of the single sheath. The ac cable effective resistance R_{ac}

$$P_t = 3I_{\text{rms}}^2 R_{ac} \tag{17}$$

leads to ac/dc ratios corresponding to (15) and (16)

$$\frac{R_{ac}}{R_{dc}} = \frac{1}{3}\left(\sum_{i=1}^{3}\frac{P_{ci}}{P_{dci}} + \sum_{i=1}^{3}\frac{P_{si}}{P_{dci}}\right) \tag{18}$$

and

$$\frac{R_{ac}}{R_{dc}} = \frac{1}{3}\left(\sum_{i=1}^{3}\frac{P_{ci}}{P_{dci}}\right) + \frac{P_s}{\sum_{i=1}^{3} P_{dci}}, \tag{19}$$

respectively, where R_{dci} and P_{dci} are the dc resistance and dc loss, respectively, per unit length of a conductor. The coupled electromagnetic diffusion equations provide the final MVP and temperature nodal values as well as the final source current densities of the three conductors. Using these values it is possible [10] to calculate the average loss density contribution of element e, given by (9). The mean value of the losses per unit length of this element will be obtained by the integration of $\dot{q}^e$ over the element cross section S^e as

$$P^e = \iint_{S^e} \dot{q}^e \, dx \, dy. \tag{20}$$

The total losses per unit length of conductor or sheath i are finally calculated as the summation of the element loss contributions of the corresponding conductor or sheath.

To compute the conductor i inductance L_{ci}, we use the mean value W_{mi} of the stored magnetic energy per unit length of this conductor

$$W_{mi} = \tfrac{1}{2} L_{ci} I_{\text{rms}}^2. \tag{21}$$

Using the integral form of this energy and taking its mean value [6], it becomes

$$W_{mi} = \tfrac{1}{2} Re\left\{J_{si}^* \iint_{S_i} A(x, y)\, dx\, dy\right\} \tag{22}$$

and the inductance of conductor i may be calculated using (21) and (22) as

$$L_{ci} = \frac{1}{I_{\text{rms}}^2} Re\left\{J_{si}^* \iint_{S_i} A(x, y)\, dx\, dy\right\}. \tag{23}$$

This inductance is related to the mean inductance of the isolated phase arrangement of Fig. 1(a)

$$L_b = \frac{\mu_0}{2\pi}\left(\ln\frac{S\sqrt[3]{2}}{r_o} + \frac{1}{4}\right) \tag{24}$$

or to the mean inductance of the three-conductors one-sheath arrangement of Fig. 2(b)

$$L_S = \frac{\mu_0}{2\pi}\left(\ln\frac{m}{r_o} + \frac{1}{4}\right) \tag{25}$$

B. Electromagnetic Forces

The force $d\vec{F}$ on the volume element dv at which the current density is $\vec{J}$ is given by

$$d\vec{F} = (\vec{J} \times \vec{B})\, dv \tag{26}$$

where, according to the assumptions, the flux density vector $\vec{B}$ will be on the x–y plane. The force per unit length acting on element e of conductor i will be equal to

$$\vec{F}_i^e = \hat{x} F_{xi}^e + \hat{y} F_{yi}^e \tag{27}$$

where

$$F_{xi}^e = -\iint_{S_i^e} J^e(x, y) B_y^e \, dx\, dy \tag{28a}$$

and

$$F_{yi}^e = \iint_{S_i^e} J^e(x, y) B_x^e \, dx\, dy \tag{28b}$$

It should be noted that in (28) the flux density as well as the force components are assumed to be constant on the cross section of element e. This assumption implies that the interpolation functions used in the FE formulation are linear polynomials in x and y (i.e., first-order shape functions). This simplifies the elementary computations that concern quantities deriving as first derivatives without introducing any error, providing that the finite elements are small enough to follow the possible step discontinuities.

Defining the phasors of the element current I^e and of the flux density B_x^e and B_y^e as

$$\begin{aligned} I^e &= I_{\text{rms}}^e e^{j\theta^e} \\ B_x^e &= B_{x\,\text{rms}}^e e^{j\varphi_x^e} \\ B_y^e &= B_{y\,\text{rms}}^e e^{j\varphi_y^e} \end{aligned} \tag{29}$$

the products of the corresponding force per unit length time functions in this element will be

$$\begin{aligned} f_x^e(t) &= -I_{\text{rms}}^e B_{y\,\text{rms}}^e [\cos(\theta^e - \varphi_y^e) \\ &\quad + \cos(2\omega t + \theta^e + \varphi_y^e)] \\ f_y^e(t) &= I_{\text{rms}}^e B_{x\,\text{rms}}^e [\cos(\theta^e - \varphi_x^e) \\ &\quad + \cos(2\omega t + \theta^e + \varphi_x^e)]. \end{aligned} \tag{30}$$

The total force time functions, that define the total force acting on conductor i, will be derived as the assembly of the elementary force contributions of this conductor

$$\begin{aligned} f_x(t) &= \sum_e f_x^e(t) \\ f_y(t) &= \sum_e f_y^e(t). \end{aligned} \tag{31}$$

These forces are related to a base force f_b equal to

$$f_b = \frac{\mu I_{\text{rms}}^2}{2\pi l} \tag{32}$$

which applies between two straight parallel conductors carrying a current I_{rms} and being at a distance $l = S$ (for the isolated phase arrangement) or at a distance $l = m/\sqrt{3}$ (for the three-conductors one-sheath arrangement).

C. Ampacity

The ampacity of a gas insulated pipe-type cable is limited only by the maximum sheath temperature. This is the result of good heat transfer through the gas insulation, that leads to a small temperature drop between conductor and sheath. This maximum sheath temperature has only to be limited so that it will not dry out the soil near the cable.

The mean temperatures of element e are used to calculate the mean temperatures T_{ci} and T_{si} of conductor i and sheath i respectively. After the termination of the iterative procedure these mean temperatures may be plotted against the cable current. If we define the maximum conductor and sheath temperature that is allowed, the cable ampacity is estimated. It should be noted that due to the thermal proximity effect in the isolated phase arrangement, the temperatures of the central conductor and sheath cable will be higher than those of the other two cables. So, these temperatures determine the cable ampacity.

VII. Results

A. Comparison with Approximate Calculations

Doepken presented in [12] the first comparison between an isolated phase and a three conductor gas cable, both having nominal voltage 230 kV. To calculate the cables ampacity, he used a thermal conductivity of the earth of 1.11 W/m°C, a sheath temperature rise of 35°C above a 25°C ambient, a load factor of 100%, sheath and conductor emissivities of 0.95 and SF_6 at 345 kPa (50 psi). The ampacities obtained in [12] were used as input in the FEM formulation of this paper and the results are shown in Table I. The difference in the total loss estimation between the two approaches in the isolated case as well as the lower sheath temperature rise obtained from FEM in both cases are due to the approximations used by Doepken. These approximations involve a loss estimation of conductor and sheath losses based on Dwight's formula [13], suffering from the assumption of a uniformly distributed current over the conductors cross-section, as well as an ampacity estimation based on [14], suffering from geometrical assumptions.

Graneau presented in [2] a more accurate method for the loss and ampacity calculation of both isolated phase and three phase-one sheath gas cables. Using his method, three different isolated phase cables were calculated and the ampacities obtained were used again as input to the FEM formulation of this paper. The results, appearing in Table II, show an excellent agreement between the two approaches. The small differences encountered here are mainly due to the 1:1 conductor-sheath current transformer assumption used by Graneau in the calculation of the sheath equivalent resistance.

B. Parameter Analysis

The large number of operational parameters involved in buried cables prevents the development of generalized charts concerning all cases. However, the FEM formulation of this paper is capable to investigate any particular arrangement. In order to illustrate this, one case referring to three-phase one-sheath cable and one referring to an isolated-phase cable were examined. In both cases the following geometrical and physical properties were common (using the notation of Fig. 1(a-b) and Fig. 2(a-b):

$$\begin{aligned}
\mu_{rc} &= 1 & \mu_{rs} &= 1 \\
\sigma_{c0} &= 3.86 \cdot 10^7 \text{ S/m} & \sigma_{s0} &= 3.75 \cdot 10^7 \text{ S/m} \\
\alpha_c &= 3.96 \cdot 10^{-3} \text{ 1/°C} & \alpha_s &= 3.96 \cdot 10^{-3} \text{ 1/°C} \\
\xi_c &= 0.3 & \xi_s &= 0.8 \\
k_c &= 150 \text{ W/m°C} & k_s &= 150 \text{ W/m°C} \\
k_a &= 0.028 \text{ W/m°C} & k_e &= 1.11 \text{ W/m°C} \\
T_{sp} &= 20\text{°C} & h &= 11.36 \text{ W/m}^2\text{°C} \\
d_c &= 0.01270 \text{ m}
\end{aligned} \tag{33}$$

The geometrical properties of the three-conductor gas cable were:

$$\begin{aligned}
r_o &= 0.06350 \text{ m} & d_s &= 0.01270 \text{ m} \\
m &= 0.25765 \text{ m} & D &= 0.85 \text{ m}
\end{aligned}$$

while the sheath radius R_i varies from 0.22 to 0.36 m. The ambient temperature T_∞ was 25°C and the cable was buried in a homogeneous soil system, i.e., the thermal conductivity of the trench backfill k_b was set equal to k_e. In Fig. 3(a) the mean temperatures of conductors and sheath are shown. The parameter is the cable rms current, ranging from 1500 A to 3000 A. This plot may give implicitly the ampacity of the cable, if the allowable sheath temperature is determined. Taking for example as an upper limit for T_s a value of 60°C, a maximum current of 2000 A for a minimum sheath radius of 0.243 m is determined. In Fig. 3(b) the ac/dc losses of the conductors and sheath defined in (19) versus R_i are shown. As it was expected, only the sheath losses present an essential variation and they also tend to a constant value as the sheath moves away from the conductors. In Fig. 3(c) the inductance of the conductor #1, for the same range of rms current, is shown. The inductances are related to the inductance L_s defined in (25). The current variation has negligible influence on the inductance, confirming the identity that inductance is only a function of geometry and μ_0. Finally in Fig. 3(d) the forces acting on the same conductor for rms current 2000 A are presented. The forces are related to the force f_b defined in (32) and they are plotted for a

TABLE I

Cable Arrangement	Ampacity [A]	R_i [m]	r_o [m]	P_t from [12] [W/m]	P_t from FEM Procedure [W/m]	$T_s - T_\infty$ [°C]
Isolated phase	1550	0.14478	0.05080	124.7	111.4	22.9
Three-conductor	1480	0.22860	0.04064	111.5	111.3	29.9

Comparison of the total loss P_t and mean sheath temperature rise between an isolated phase gas cable and a three conductor gas cable as obtained by the coupled FEM procedure, with the corresponding calculation of [12]. The ampacities in [12] were calculated for a 35°C sheath temperature rise T_s above a 25°C ambient temperature T_∞. In both cases the conductor wall thickness d_c was 0.01270 m, the sheath wall thickness d_s was 0.00762 m and the depth of burial of cable axis below ground level D was 0.91440 m. The spacing S of the isolated phase cables was 0.45 m while the distance between conductor centres m of the three conductor case was 0.19558 m.

TABLE II

Voltage [kV]	r_o [m]	R_i [m]	d_s [m]	S [m]	Ampacity from [2] [A]	P_t [W/m]	P_t from FEM procedure [W/m]	T_s [°C]
145	0.0445	0.1141	0.0064	0.34	1560	141.0	138.9	59.0
362	0.0635	0.1829	0.0076	0.56	2313	187.5	187.4	61.2
550	0.0890	0.2476	0.0064	0.71	2940	227.4	228.5	62.9

Comparison of the total loss and temperature values of 3 different isolated-phase gas cables as obtained by the coupled FEM procedure, with the corresponding approximating method of Graneau [2]. The ampacities shown in the table were calculated for 40°C sheath temperature rise above a 20°C ambient temperature and with soil conductivity k_e = 1.11 W/m°C. In all cases the conductor wall thickness d_c was 0.0127 m and the depth of burial D was 0.91 m.

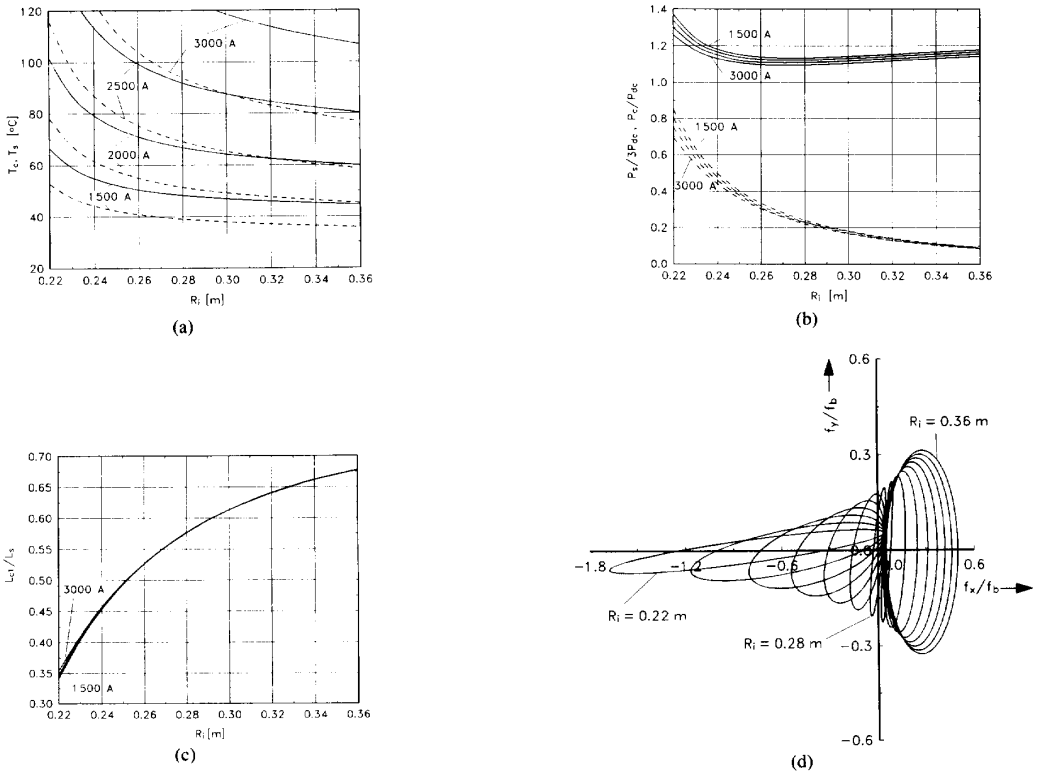

Fig. 3. (a) Conductor (solid lines) and sheath (dashed lines) mean temperatures T_c and T_s respectively versus sheath radius R_i. (b) Conductor (solid lines) and sheath (dashed lines) ac/dc loss ratios versus sheath radius R_i. (c) Conductor #1 inductance versus sheath radius R_i. (d) Conductor #1 forces versus sheath R_i, for I_{rms} = 2000 A.

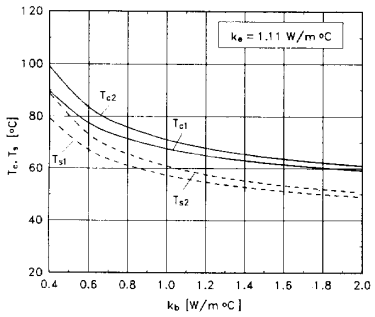

Fig. 4. Conductor (solid lines) and sheath (dashed lines) mean temperatures of left (T_{c1} and T_{s1}) and middle (T_{c2} and T_{s2}) cables respectively versus backfill thermal conductivity k_b, for the isolated-phase arrangement.

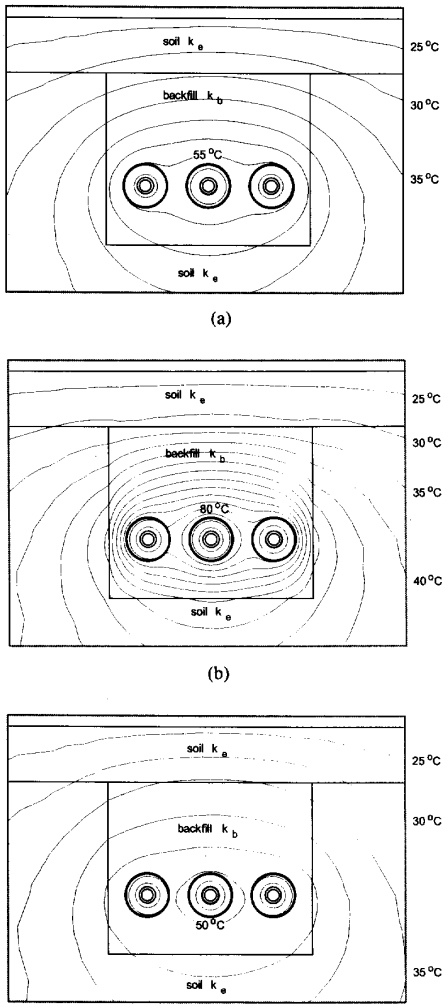

Fig. 5. Temperature contours of the 145 kV isolated-phase gas insulated cable for I_{rms} = 1560 A buried in a trench that is filled with three different backfill materials: (a) Homogeneous soil system, i.e., $k_b = k_e = 1.11$ W/m°C. (b) $k_b = 0.4$ W/m°C. (c) $k_b = 2.0$ W/m°C. The contours are plotted with step equal to 5°C and the soil T_{sp} and ambient T_∞ temperatures are both equal to 20°C.

time variation equal to a half period. It is known [15] that the locus of the force vector for this time variation is a real ellipse. There is always a lower limit of sheath radius (in this case 0.29 m) below which the forces have a substantial negative x-component. This component is dangerous and has to be avoided, because during short circuit conditions it may cause deflection and vibration of the conductors.

The isolated-phase gas cable that was examined has the geometrical properties and the ampacity of the 145 kV cable of Table II and the ambient temperature T_∞ was 20°C. In this case a trench of variable thermal conductivity k_b was considered, with dimensions given by $Y = 1.23$ m and $W = 1.10$ m (see Fig. 1(b)). The top 0.30 m of this trench was assumed to be filled with native soil, having the same thermal conductivity as the rest of the outside domain, i.e., k_e. In Fig. 4 the temperatures of the conductor and sheath located in the middle (cable #2) as well as one of the outside cables (cable #1) are shown as a function of k_b. The gain in the allowable heat input and hence in the cable's ampacity is very significant when the backfill's thermal conductivity rises. This figure shows clearly the potential benefits to be achieved through development of backfill materials with high thermal conductivity. Finally, in Fig. 5(a-c), the temperature contours of the same cable with rms current 1560 A and for three different backfill materials are shown, illustrating the previous conclusion.

VIII. Conclusions

The FE formulation presented in this paper leads to an efficient computation of the coupled magneto-thermal field in both isolated phase and three-phase gas insulated cables. The calculation of an equivalent thermal conductivity of SF_6 leads to a conduction based thermal diffusion equation. There are no other approximations concerning the cable geometry and the electromagnetic and thermal properties of the involved materials. The problem is solved using a very fast iterative procedure. From the field computation, the cable losses and ampacity along with the forces and conductor inductances are easily obtained.

References

[1] R. Hess, W. Lehmann, F. Richter, H. H. Schramm, and G. Hosemann, "Control of high normal and short-circuit currents in SF_6-insulated substations," *CIGRE Rep. 32-07*, 1978.

[2] P. Graneau, *Underground Power Transmission*, New York: Wiley, 1979.

[3] V. Hatziathanassiou and D. Labridis, "Coupled magneto-thermal field computation in three-phase gas insulated cables. Part 1: Finite Element Formulation," *Arch. Elektrotech.*, vol. 76, no. 4, pp. 285-292, May 1993.

[4] J. Weiss and Z. Csendes, "A one-step finite element method for multiconductor skin effect problems," *IEEE Trans. Power App. Syst.*, vol. PAS-101, no. 10, pp. 3796-3803, Oct. 1982.

[5] P. Silvester and R. Ferrari, *Finite Elements for Electrical Engineers*, Cambridge: Cambridge University Press, 1984.

[6] D. Labridis and P. Dokopoulos, "Finite element computation of field, losses and forces in a three-phase gas cable with non-symmetrical conductor arrangement," *IEEE Trans. Power Delivery*, vol. PWDR-3, no. 4, pp. 1326-1333, Oct. 1988.

[7] V. K. Garg, J. Weiss, R. M. Del Vecchio, and J. Raymond, "Magneto-thermal coupled finite element calculations in multiconductor systems," *IEEE Trans. Magn.*, vol. MAG-23, no. 5, pp. 3296-3298, Sept. 1987.
[8] F. P. Incropera and D. P. De Witt, *Fundamentals of Heat and Mass Transfer*, New York: Wiley, 1990.
[9] H. C. Doepken, Jr., "Calculated heat transfer characteristics of air and SF_6," *IEEE Trans. Power Appar. Syst.*, vol. PAS-89, no. 8, pp. 1979-1985, Nov.-Dec. 1970.
[10] V. Hatziathanassiou and D. Labridis, "Coupled magneto-thermal field computation in three-phase gas insulated cables. Part 2: Calculation of Ampacity and Losses," *Arch. Elektrotech.*, vol. 76, no. 5, pp. 397-404, June 1993.
[11] A. Konrad, "Integrodifferential finite element formulation of two-dimensional steady-state skin effect problems," *IEEE Trans. Magn.*, vol. MAG-18, no. 1, pp. 284-292, Jan. 1982.
[12] H. C. Doepken, "Compressed-gas-insulated cables with increased ampacity and reduced cost," IEEE Conference Record: 1974 Underground T and D Conference, pp. 536-540, 1974.
[13] H. B. Dwight, "Proximity effect in cable sheaths," *AIEE Trans.*, vol. 50, pp. 993-998, Sept. 1931.
[14] B. L. Johnson, H. C. Doepken, and J. G. Trump, "Operating parameters of compressed-gas-insulated transmission lines," *IEEE Trans. Power Appar. Syst.*, vol. PAS-88, no. 4, pp. 369-375, Apr. 1969.
[15] D. Labridis, "Solution of the nonlinear multiconductor problem with the finite element method," Ph.D. Dissertation, Department of Electrical Engineering, Aristotelian University of Thessaloniki, Greece, September, 1989.
[16] P. Silvester and M.-S. Hsieh, "Finite-element solution of 2-dimensional exterior-field problems," *IEE Proc.*, vol. 118, no. 12, pp. 1743-1747, Dec. 1971.
[17] P. P. Silvester, D. A. Lowther, C. J. Carpenter, and E. A. Wyatt, "Exterior finite elements for 2-dimensional field problems with open boundaries," *IEE Proc.*, vol. 124, no. 12, pp. 1267-1270, Dec. 1977.
[18] S. J. Salon and J. M. Schneider, "A hybrid finite element-boundary integral formulation of the eddy-current problem," *IEEE Trans. Magn.*, vol. MAG-18, no. 2, pp. 461-466, Mar. 1982.
[19] H. Hurwitz, Jr., "Infinitesimal scaling—A new procedure for modeling exterior field problems," *IEEE Trans. Magn.*, vol. MAG-20, no. 5, pp. 1918-1923, Sept. 1984.
[20] M. V. K. Chari and G. Bedrosian, "Hybrid harmonic/finite element method for two-dimensional open boundary problems," *IEEE Trans. Magn.*, vol. MAG-23, no. 5, pp. 3572-3574, Sept. 1987.
[21] E. Tarasiewicz, E. Kuffel, and S. Grzybowski, "Calculation of temperature distribution within cable trench backfill and the surrounding soil," *IEEE Trans. Power App. Syst.*, vol. PAS-104, no. 8, pp. 1973-1978, Aug. 1985.
[22] G. J. Anders, M. Caaban, N. Bedard, and R. W. D. Ganton, "New approach to ampacity evaluation of cables in ducts using finite element technique," *IEEE Trans. Power Del.*, vol. PWDR-2, no. 4, pp. 969-975, Oct. 1987.
[23] J. Weiss, V. K. Garg, and E. Sternheim, "Eddy current loss calculation in multiconductor systems," *IEEE Trans. Magn.*, vol. MAG-19, no. 5, pp. 2207-2209, Sept. 1983.
[24] E. Tarasiewicz and J. Poltz, "Mutually constrained partial differential and integral equations for an exterior field problem," *IEEE Trans. Magn.*, vol. MAG-19, no. 6, pp. 2307-2310, Nov. 1983.

Dimitris Labridis (S'88-M'90) was born in Thessaloniki, Greece, on July 26, 1958. He received the Dipl.-Eng. degree and the Ph.D. degree from the Department of Electrical Engineering at the Aristotelian University of Thessaloniki, in 1981 and 1989, respectively.

During 1982-1989 he has been working as a research assistant at the Department of Electrical Engineering at the Aristotelian University of Thessaloniki, Greece. Since 1990 he is a Lecturer in the same Department. His special interests are power system analysis with special emphasis on the simulation of transmission and distribution systems, electromagnetic field analysis and numerical methods in engineering.

Vassilis Hatziathanassiou was born in Serres, Greece, on October 30, 1954. He received the Dipl.-Eng. degree and the Ph.D. degree from the Department of Electrical Engineering at the Aristotelian University of Thessaloniki, in 1978 and 1988, respectively.

During 1980-1989 he has been working as a research assistant at the Department of Electrical Engineering at the Aristotelian University of Thessaloniki, Greece. Since 1990 he is a Lecturer in the same Department. His special interests are thermodynamics, heat transfer and electric power stations.